CLRC

Charge Storage Effects in some Avalanche Photodiodes Proposed for use in the CMS ECAL

J E Bateman and R Stephenson

CHARGE STORAGE EFFECTS IN SOME AVALANCHE PHOTODIODES PROPOSED FOR USE IN THE CMS ECAL

J E Bateman and R Stephenson
Rutherford Appleton Laboratory, Chilton, Didcot, OX11 0QX, UK

In the course of calibrating a large number of avalanche photodiodes for the 1995 ECAL beam tests we noted a surprising spread in the apparent gains of the devices. We report that this effect seems to be due to charge storage in the devices causing a variable ballistic deficit in our pulse-shaping circuit.

1. INTRODUCTION

At RAL we have been responsible for the development and commissioning of the front-end electronics (charge preamplifier, shaper amplifier and bias supplies) and the physical packaging for the avalanche photodiode (APD) readout of the test module of the CMS lead tungstate ECAL tested at CERN in 1995. (Figure 1 shows a schematic diagram of the amplifier.) In the course of this programme we tested 20 modules equipped with EG&G APDs (type # C30719E) and 36 Hamamatsu devices (type # S5345). This exercise, while limited in its scope by the need to do it against the clock, did provide some reasonable statistics on the performance of the APD readout modules (reported in reference [1]). Most disturbing of our findings was that for both types of APD the apparent gains were spread over a range of about 2.5:1 when the bias value was set to that given by the manufacturer as yielding a nominal gain of 50.

In our commissioning tests a blue (485nm peak) light emitting diode (LED) was mounted in a fixed position opposite the APD and driven by a 12ns wide pulse of about 40V. All conditions were kept rigorously constant during the sequence of measurements. The main variation expected was from changes in ambient temperature. However, the very stable weather pattern at the time resulted in the range of temperature remaining within $\pm 1C$ for the whole period. Self heating of the modules was also a source of variation, however the built-in temperature monitor on each unit enabled us to limit the temperature variation to around $\pm 1C$. We therefore anticipated a maximum spread in the measured pulse heights (i.e. gains) of $\approx 20\%$. Each APD was biased to the manufacturer's specified value for a gain (M) of 50. Figure 2 shows a histogram of the peak pulse heights measured for the 20 EG&G diodes and figure 3 the equivalent histogram for the Hamamatsu diodes. The EG&G devices are fairly uniformly spread over a range of $\approx 2.5:1$ while the Hamamatsu devices show a compact core with a fair number of outliers again reaching a range of $\approx 2.5:1$. A further finding from these results is that the mean of the EG&G distribution is only 70% of the mean of the Hamamatsu distribution (both having a nominal gain of 50).

We also measured the full width at half maximum (FWHM) of the LED-induced pulse height distributions for each diode and the FWHM of the white noise which was subtracted in quadrature to yield the root mean square (RMS) noise of the LED-induced pulse height distribution. In figure 4 we see the fractional RMS resolution (squared) plotted against the peak pulse height for all the APDs tested. According to the elementary statistical model the results should cluster around a single spot with a pulse amplitude corresponding to a gain of 50 and a "y" value of F/N where F is the excess noise factor and N is the number of initial photoelectrons generated in the front of the APD. Or rather, following the measurements of the Ecole Polytechnique group [2] we might expect to see two clusters resulting from the different observed F values for the two types of diode. As figure 4 shows we observe a distribution which shows a linear improvement in resolution with increasing pulse height. The two diode types overlap in the distribution, but the Hamamatsu show, on average, a higher pulse height and a better resolution.

A clue to the possible source of these effects was observed in the form of a long ($\approx \mu s$) tail observed on LED-induced pulses which was not consistent with the ballistic response of our 30ns CR-RC shaping circuit. We therefore decided to examine the fundamental pulse waveforms originating from the APDs to see if anything could be learned. Fortunately we

were left with a small sample of three of each type of APD with which to carry out these investigations.

2. EXPERIMENTAL MEASUREMENTS

In order to inspect the pulse waveform delivered by an APD we simply extracted a connection (via a line-terminating resistor) from the output of the buffer in figure 1 (U011 pin 1) i.e. before the shaping amplifier. As a first exercise we looked at the ratio of the observed pulse heights from two EG&G devices which showed a large gain difference with our standard circuit. By connecting the signal from the buffer to an Ortec 575 pulse amplifier we could get shaping time constants (CR-RC) of 0.5, 1.5 and $3\mu s$ in addition to our standard value of 30ns. Figure 5 shows the ratio of the pulse heights as a function of the shaping time. Clearly the ratio tends approximately to unity as the time constant increases.

Figure 5 tended to confirm our suspicion that the gain values supplied by the APD manufacturers are measured at DC (or very low frequency). Performing a DC gain measurement on the samples in our hands produced accurate agreement with the gain figures supplied by the manufacturers. (We read the plateau photocurrent before avalanching commenced as corresponding to unity gain in the diode.)

Inspection of the basic charge-loop waveforms on an oscilloscope immediately disclosed some very long time constants in the waveform delivered by the APDs. The presence of the white noise made precise measurements impossible (particularly in the case of the Hamamatsu diodes) so for accurate data a LeCroy 9450 (350Mhz analogue bandwidth) digital oscilloscope was used in signal-averaging mode. An average of 1000 frames was used in all cases. Figure 6 shows the waveforms observed from three EG&G APDs. The ballistic response of the charge preamplifier is shown by the response to a injected step fuction of 10^6 electrons. The waveforms have been normalised together at the longest time $(9\mu s)$ on the assumption that all the charge should have been collected by this time. Not only do we observe some very slow (μs) time constants but the distribution of charge between the time constants is very variable.

Illuminating an APD with a fast red-emitting LED (635nm peak) can (because of the longer attenuation length of the light in silicon) show up structure-dependent features of the APD design. Figure 7 shows the waveforms observed from EG&G #135 with blue and red light. There is clearly a dramatic difference in the response.

A measure of the charge-delivery from the APD can be obtained by normalising the LED-induced waveforms to the test-pulse waveform. Figure 8 shows the results of this procedure applied to the waveforms from the three EG&G devices. It is clear that the the waveforms fit very well to a three-time constant model with a very fast (tens of ns) component, a component of around $0.5\mu s$ and a third one of around $5\mu s$. However, it is clear that the fraction of signal in each component (and the exact values of the time constants) are subject to great variation. The fraction of the signal in the fast time constant varies between 14% and 54%.

Repeating the measurements with the three Hamamatsu diodes we observe similar results, but as figure 9 shows, the variability between the samples is very much less (at least in the case of the three diodes sampled) than in the case of the EG&G devices. The response of Hamamatsu #27 to the red LED is indistinguishable from the response to the test pulser (i.e. the charge delivery is faster than the response of the amplifier).

Normalising the blue-LED response waveforms to the amplifier response reveals excellent single time constant fits with much less variability than observed with the EG&G diodes. Approximately 85-90% of the signal is in the fast part of the signal and the slow time constant is around $1\mu s$ (figure 10).

In order to be confident that the slow times constants are a feature of the APD response and not a feature of the blue LED output, the blue LED signal was used to irradiate an RCA 8575 (fast linear) photomultiplier tube. The anode of the tube was connected straight to a fast oscilloscope and terminated in 50Ω. The resulting waveform is plotted in figure 11. With >95% of the light delivered in 60ns, the LED does not contribute to the slow time constants observed in the APD output.

3. DISCUSSION

While our sample of the two populations of APDs is restricted, the results presented above permit a reasonable interpretation to be made of the gain variations observed in the total population. The 30ns shaping time constants of our circuit will clearly only pass the fastest component of the APD waveform with high efficiency. In the case of the EG&G diodes this automatically leads to a gain ratio of order 54.0/14.4 (figure 8) or 3.75 for #141/#135. (The observed ratio of 2.4 shows that some of the next fastest component is also contributing.) The variability of the fast component between the three samples makes the variability of the (pulse) gain seen in figure 2 no surprise. The limited sample of Hamamatsu diodes shows a very much more restricted range of fluctuation in the fast component certainly not enough to account for the extreme gain range observed in figure 3. We can only conclude that our sample of three belongs to the core distribution of figure 3 and does not contain any outliers. The fact that the Hamamatsu diodes produce bigger pulses on average than the EG&G ones is obviously due to the large component of fast signal in the former ($\approx 85\%$) compared with the latter ($<50\%$), though poor sample statistics prevent an accurate comparison.

The scatter of the points in figure 4 is also now interpretable. Low pulse heights arise by the loss of primary signal which arrives too late to be included in the pulse, thus N is smaller than it should be and the fractional RMS resolution is bigger than it should be and correlates with a low pulse height. The EG&G devices occupy the left hand portion of the field because their ballistic deficit is, in general, worse than that of the Hamamatsu diodes.

We have attempted to understand the APD waveforms in terms of a simple model of an APD. Figure 12 shows a schematic section through a "reverse" APD such as the EG&G device and (as far as the input face is concerned) we expect it to apply also to the Hamamatsu design. "W" is a heavily doped front electrode layer in which any converted photoelectrons will experience very low electric fields and travel slowly; "C" is a fully depleted conversion zone which should be thick enough to permit all photons to convert to photoelectrons and in

which the electric field is strong enough to sweep the electrons into the avalanche region ("A") in a few nanoseconds; "D" is a fully depleted drift region of sufficient depth to reduce the capacitive loading of the narrow drift region on the charge amplifier, but with a sufficiently high electric field to sweep all the avalanche electrons across it in less than 10ns; "B" is a highly doped back contact layer.

Our attention focusses on the window layer W through which the incident photons must pass. At 485nm the attenuation length of light in silicon is 0.82μm; if we assume that the conversion depth (C) is great enough to absorb all the light reaching it, and if we also assume that conversion in the window does not result in the recombination of carriers but simply in temporary trapping, we can estimate that the fast part of the pulse is simply that penetrating to the conversion zone. Then the fast fraction is simply $e^{(-W/L)}$ (where L is the attenuation length of 0.82μm). Table 1 shows the fast fractions and the corresponding values of W for the six diodes tested. The EG&G devices show W ranging from 0.5μm to 1.6μm and the Hamamatsu have 0.08μm $< W < 0.128\mu$m.

Turning to the waveforms observed with the red LED (L=4.4μm) we have some cross-check on our interpretation. In EG&G#135 we measure W=1.59 which would predict that with the red light the fast component should represent 0.696 of the total signal (assuming all the red light is stopped in the conversion zone). In fact we measure a fraction of 0.595; if we interpret the deficit as being due to the failure of the conversion zone to stop all the light we can use this number to estimate the value of C as 8.54μm.

Applying the same reasoning to the red LED waveform of Hamamatsu #27, from the blue light measurement W=0.128μm we predict a fast fraction of 0.971. This is unity within our errors of measurement and explains why the red LED waveform is indistinguishable from the ballistic response of the amplifier.

The above results are consistent with the conclusion that both types of APD possess significant window regions from which electrons escape only slowly in addition to the conversion region proper through which the electrons can travel swiftly to the avalanche region. A further check on this concept can be made by irradiating the devices with 5.9keV X-rays. These have an attenuation length of 20μm in silicon (and so can penetrate the distances in question) and the range of the delta ray produced on interaction is a small fraction of a μm so permitting sampling of the charge collection properties of a localised region. The Lecroy oscilloscope was employed in single shot mode to capture individual pulse waveforms. Figures 13 and 14 show examples of the two distinct waveforms observed from EG&G #135. Figure 13 shows a ballistic pulse that one can interpret as having converted in the conversion zone and figure 14 one that had converted in the window. A tally of about 100 events showed an approximately 50/50 sharing between the two types of events. This indicates that the window and the conversion zone are of approximately the same width i.e. $\approx 1.6\mu$m. This estimate for C is very much smaller than that obtained from the red light. The latter is almost certainly an over estimate since the red light can continue to generate useful signal through the avalanche region and into the drift region.

A test on EG&G #135 was made to see if the charge waveform was dependent on the bias potential (and thus gain). No effect was found; which tends to confirm that the charge storage is a feature of the device structure rather than biasing conditions.

4. CONCLUSIONS

The variable pulse gains observed in both EG&G and Hamamatsu APDs have been traced to the effect of ballistic deficits in our 30ns (CR-RC) shaping amplifier circuits caused by variable charge storage effects in the APDs.

In the EG&G devices we have observed fast fractions (i.e. useful response) as low as 14% of the total signal with time constants as slow as $10\mu s$.

In the Hamamatsu sample the fast fraction ranged from 86% to 90% with a slow time constant of $\approx 1\mu s$. The implication of our limited sample is that we have not seen the worst cases of this type of APD.

A simple model shows that these effects are consistent with the presence of window layers (which hold up the charge) of up to $1.6\mu m$ in the case of the EG&G devices and $0.13\mu m$ in the case of the Hamamatsu devices.

The gain measurements supplied by the manufacturers are clearly made at DC or low frequency when the storage effects are not observed. Equally, any method of measuring the excess noise factor at low bandwidths must be of limited relevance to the performance of the APD in fast pulse mode.

The presence of slow time constants in the APD signal is of great concern in the context of operation in the CMS ECAL. The demand for a very high dynamic range (10^5:1) means that base line deviations would become serious at very moderate rates.

We would suggest that the presence of these storage effects in the APDs presently to hand would probably make their use in the CMS ECAL untenable. From the small samples studied the Hamamatsu devices seem considerably better in this respect than the EG&G diodes. However, a reliable answer will require the study of a very much larger sample. Clearly, this problem is very much related to the short interaction length of blue light; however, the use of a longer wavelength has little attraction since the nuclear diode effect would increase.

REFERENCES

[1]   Survey of the performance data obtained from the commissioning of 56 channels of APD readout for the August beam tests for the CMS ECAL, J E Bateman, R Stephenson and A S Marsh

[2]   Investigation of avalanche photodiodes for EM Calorimeter at LHC, A Karar, Y Musienko, R Tanaka and J C Vanel, IN2P3-CNRS, CMS-TN / 95-095

FIGURE CAPTIONS

1.   Schematic circuit diagram of the charge preamplifier / shaper amplifier developed at RAL for the CMS ECAL tests.

2.   The distribution of mean pulse heights induced in 20 channels of ECAL readout equipped with EG&G C30719E APDs by the light pulses from a blue (485nm) LED pulse.

3.   The distribution of mean pulse heights induced in 36 channels of ECAL readout equipped with Hamamatsu S5345 APDs by the light pulses from a blue (485nm) LED pulse.

4.   A plot of the square of the fractional RMS resolution observed from the whole cohort of ECAL channels as a function of the observed peak pulse height in each case. The white noise has been subtracted (in quadrature) in each case. The channels were illuminated by a blue LED pulse of constant amplitude.

5.   A plot of the ratio of the shaped pulse heights observed in EG&G APDs #141 and #135 as a function of the shaping time constant when they are illuminated by the same blue LED light pulse. (Measured on an oscilloscope.)

6.   The signal-averaged waveforms observed at the output of the charge preamplifier of figure 1 using a Lecroy 9450 digital oscilloscope when EG&G APDs are illuminated by a blue LED pulse.

7.   A comparison of the charge waveforms observed in the APD EG&G #135 when illuminated by blue (485nm) and red (635nm) LED pulses.

8.   A plot of the waveforms of the three EG&G APDs normalised to the charge waveform to reveal the charge delivery profile of the APDs.

9.   The signal-averaged charge waveforms observed in the three Hamamatsu APDs when exposed to a blue LED light pulse (and in the case of #27) a red light pulse as well.

10. A plot of the normalised charge waveforms (blue light) of the three Hamamatsu diodes. The slow part of the charge delivery by the APDs fits very well to a single exponential time constant of around $1\mu s$.

11. The oscilloscope trace of the response of a fast photomultiplier to the blue LED light pulse used to test the APDs.

12. Schematic section of the structure of a "reverse" APD. See text for details.

13. A single shot oscilloscope trace of a "fast" 5.9keV X-ray-induced pulse in APD EG&G #135 (Lecroy digital oscilloscope).

14. A single shot oscilloscope trace of a "slow" 5.9keV X-ray-induced pulse in APD #EG&G #135 (Lecroy digital oscilloscope).

TABLE 1

Type	No.	Fast Fraction (Blue Light)	Window (μm)
EG&G	005	0.191	1.36
EG&G	135	0.144	1.59
EG&G	141	0.540	0.506
Hamamatsu	27	0.856	0.128
Hamamatsu	48	0.907	0.080
Hamamatsu	49	0.866	0.118

FIGURE 1

FIGURE 2

20 EG&G APDs

M=50   T=24C +/-1C

Mean = 1.232e5
σ = 0.315

Frequency

Pulse Height (electrons)

FIGURE 3

36 Hamamatsu
300pF APDs

M = 50   T = 24C +/-1C

Mean = 1.746e5
σ = 0.397e5

Frequency

Pulse Height (electrons)

FIGURE 4

$\sigma f^2 = F/N$
(N = constant)

- ▽ EG&G APDs
- ○ Hamamatsu APDs (300pF)

(Fractional RMS Resolution)^2 vs. Pulse Height (e-)

FIGURE 5

Ratio of P/Hs (APD #141 / APD #135) vs. Main Amplifier Shaping Time (μS)
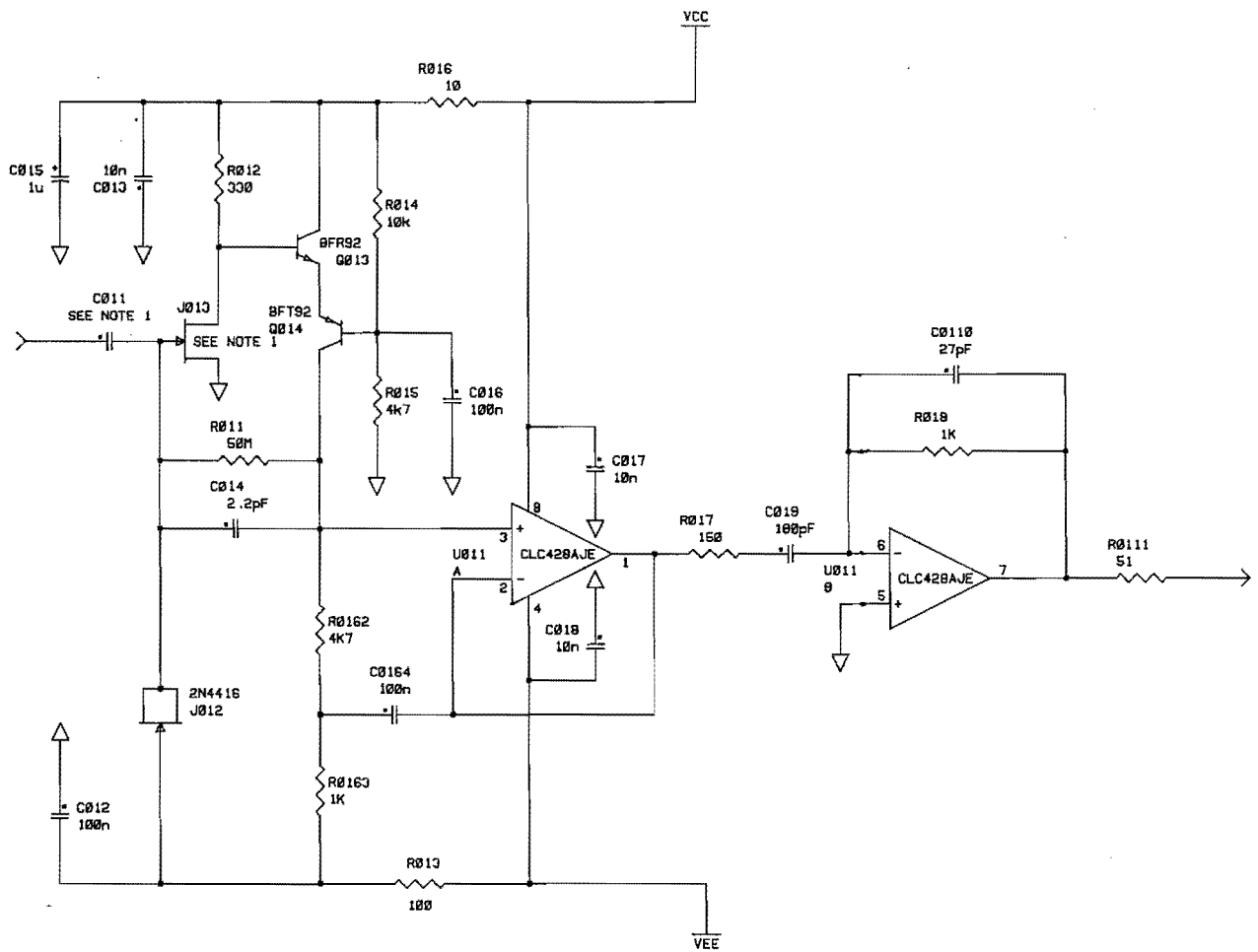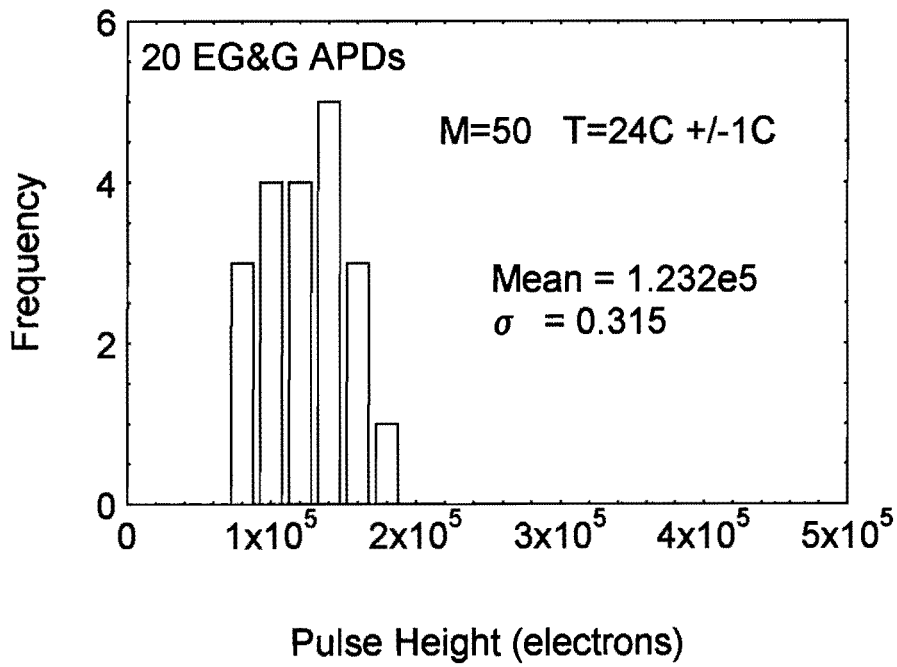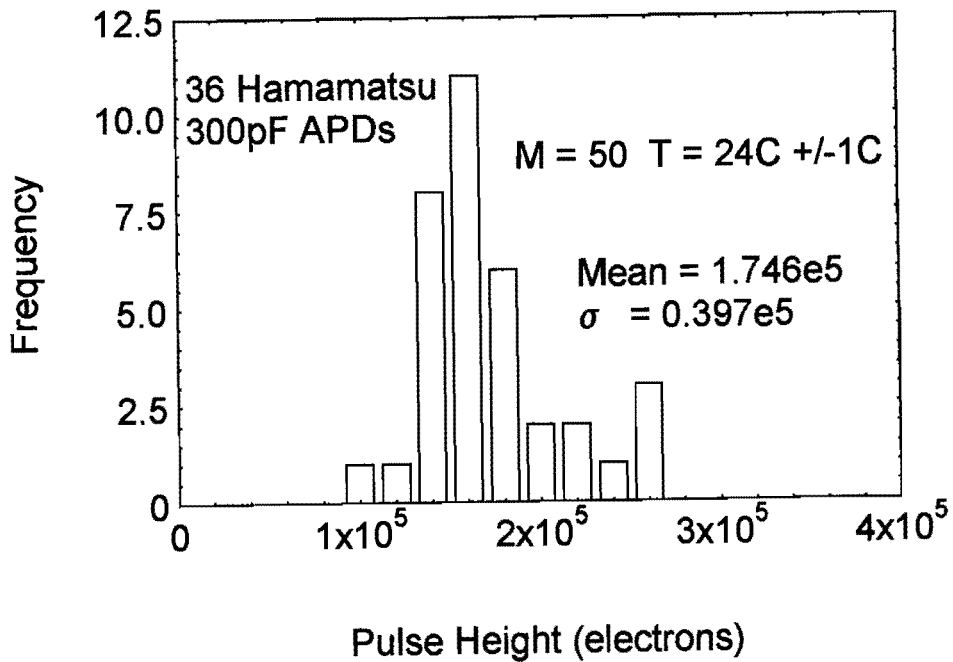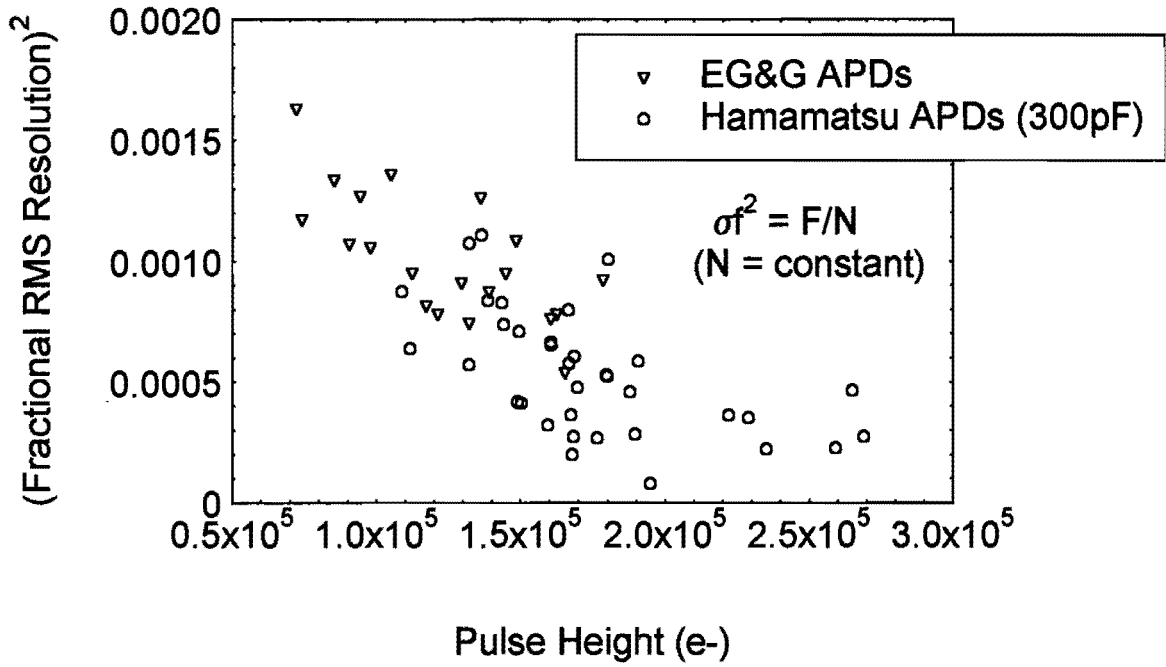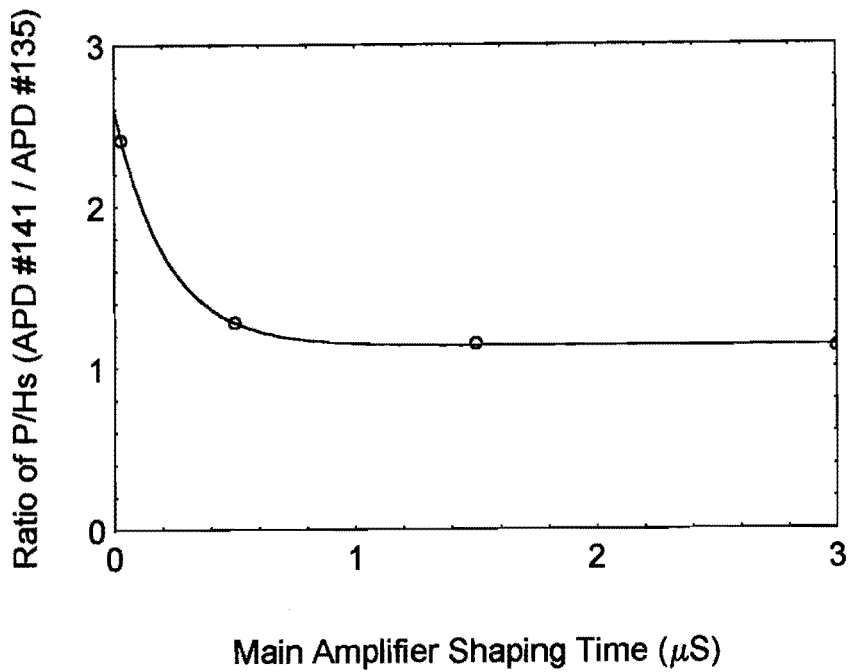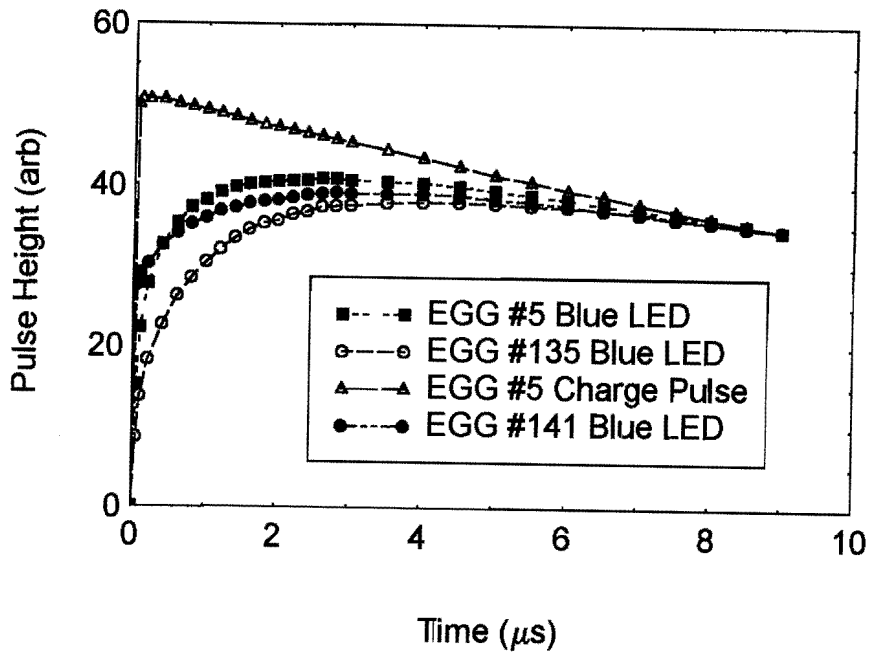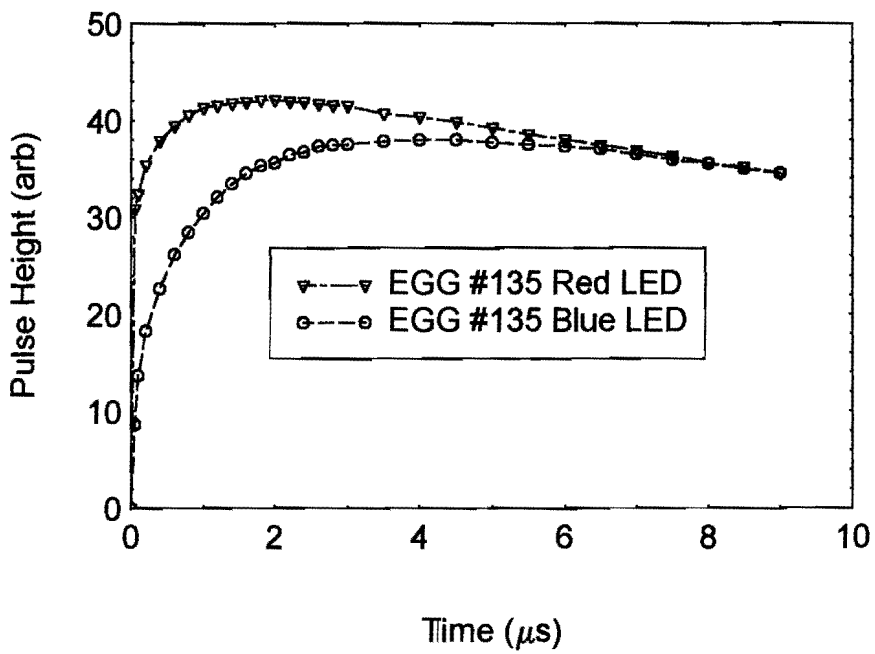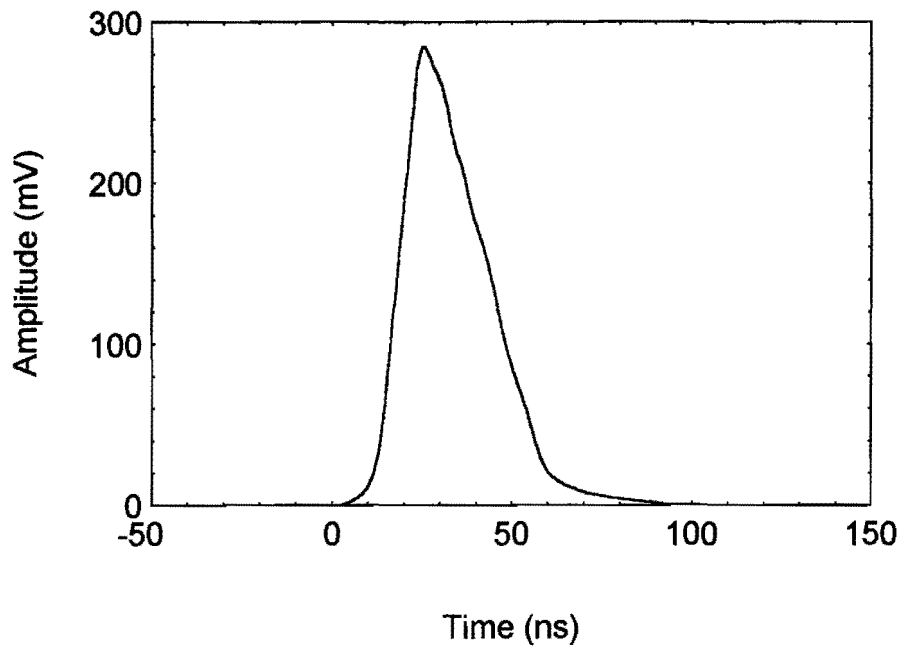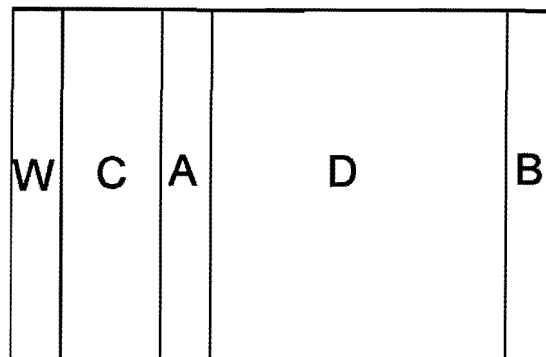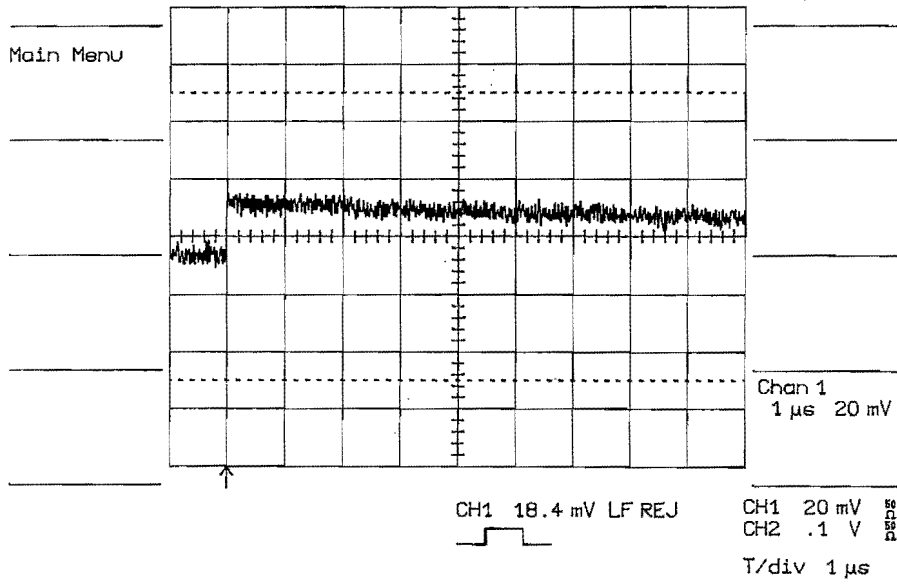
FIGURE 6

FIGURE 7

FIGURE 8
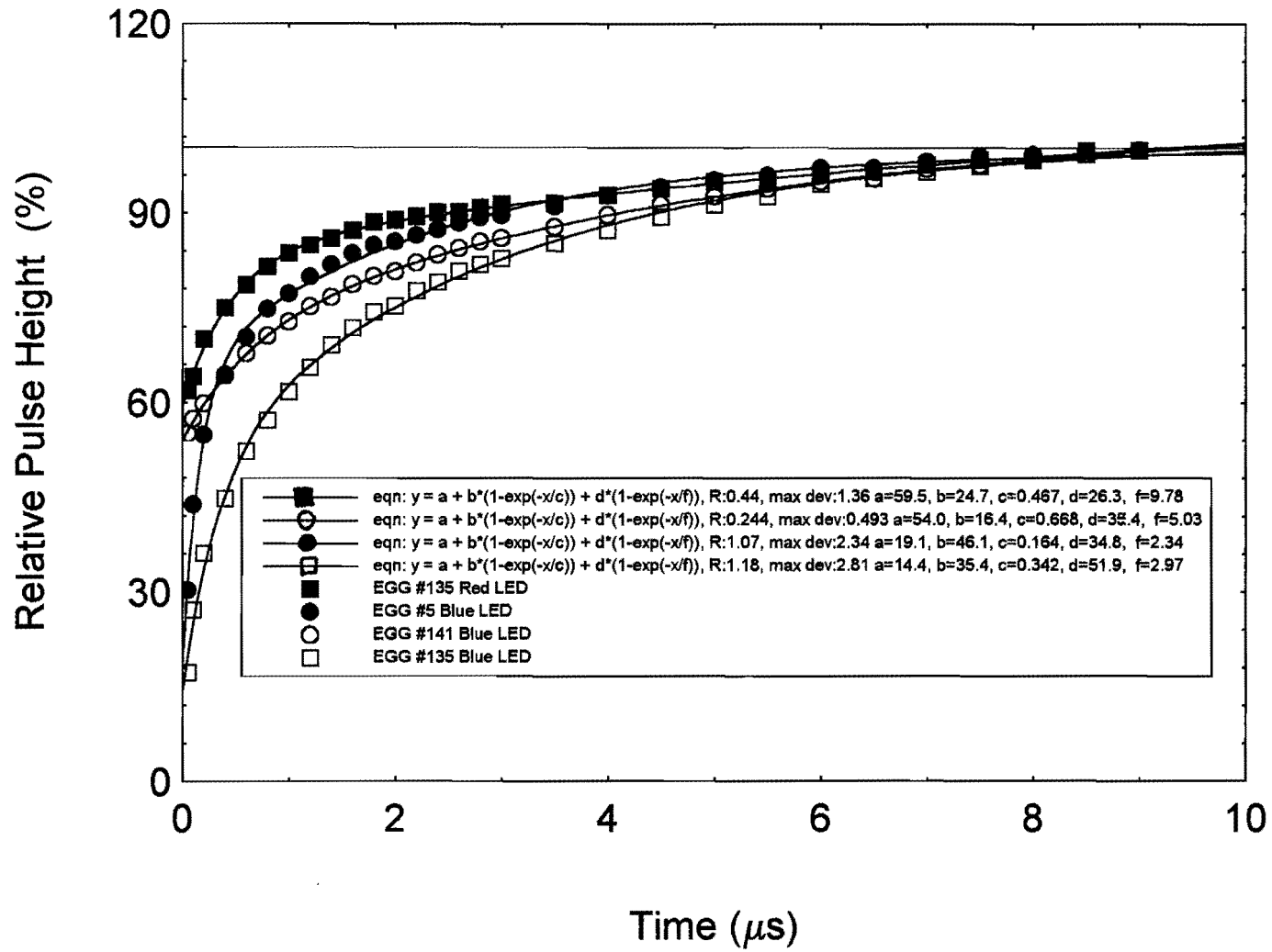
FIGURE 9
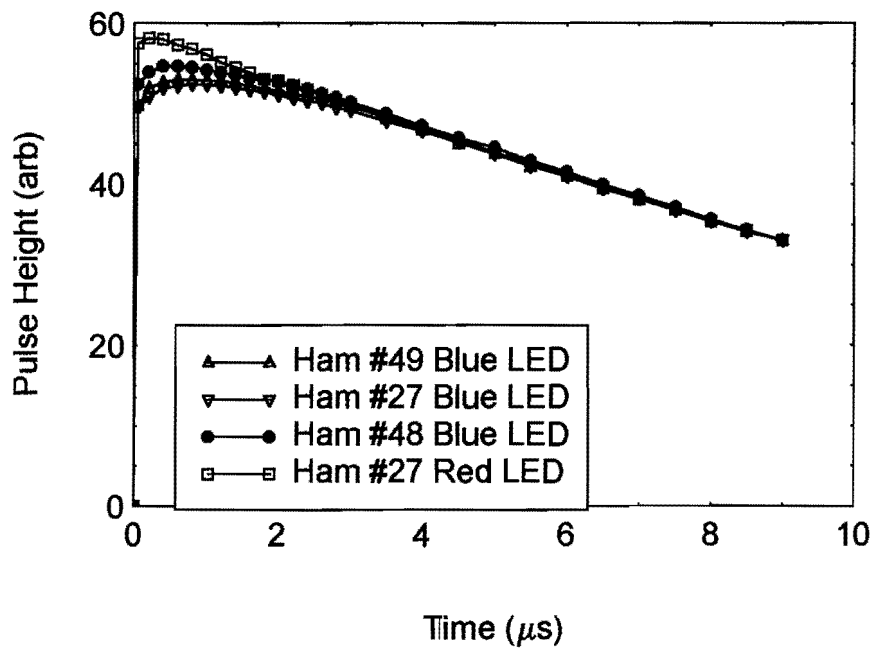
FIGURE 10
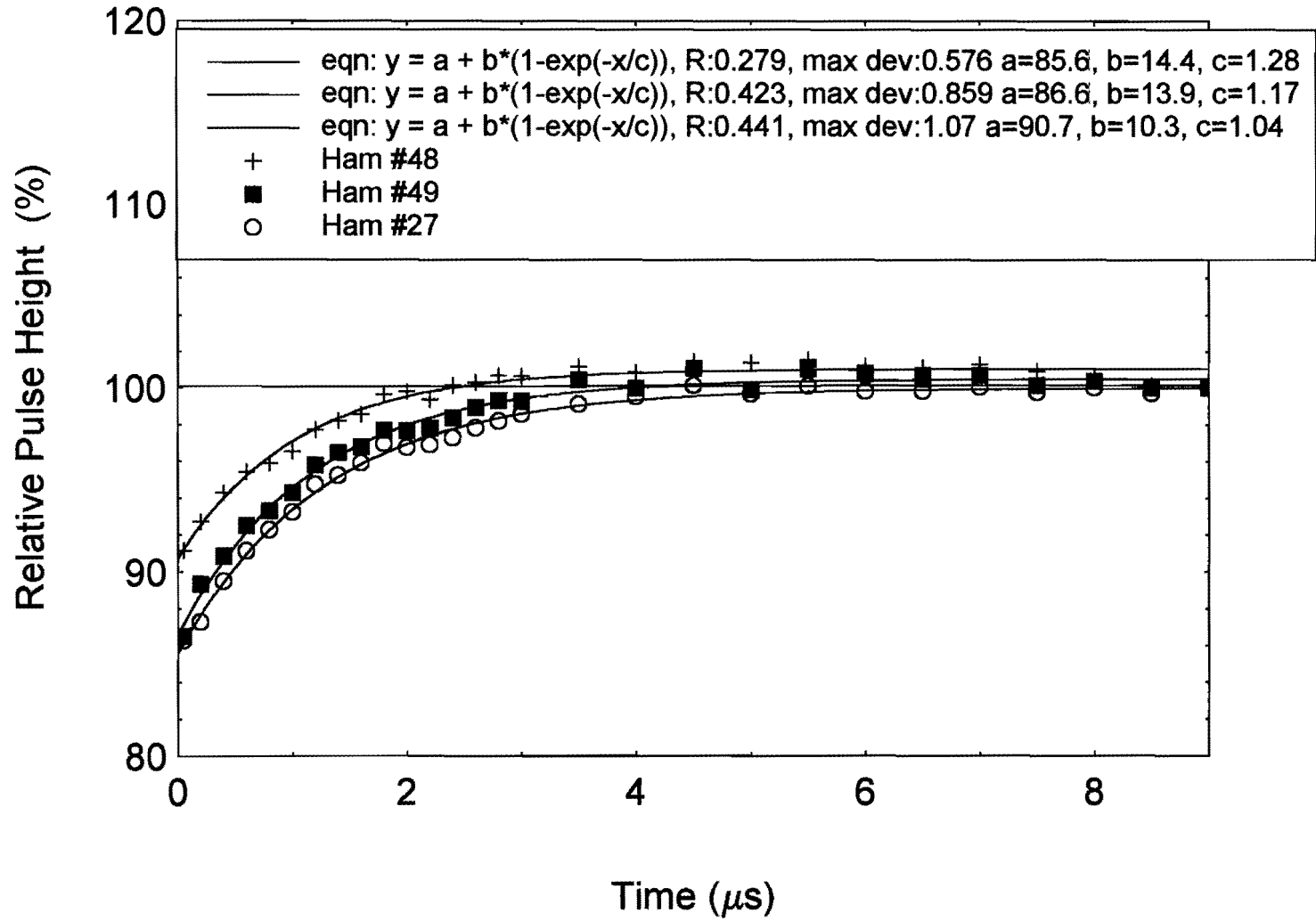
FIGURE 11

FIGURE 12

FIGURE 13

Main Menu

Chan 1
1 µs   20 mV

CH1   18.4 mV LF REJ

CH1   20 mV
CH2   .1 V

T/div 1 µs

FIGURE 14

Main Menu

Chan 1
1 µs   20 mV

CH1   18.4 mV LF REJ

CH1   20 mV
CH2   .1 V

T/div 1 µs